

# Learning to Control Physically-simulated 3D Characters via Generating and Mimicking 2D Motions

Jianan Li<sup>1</sup> Xiao Chen<sup>1</sup> Tao Huang<sup>2,3</sup> Tien-Tsin Wong<sup>4</sup>

<sup>1</sup> The Chinese University of Hong Kong <sup>2</sup> Shanghai AI Laboratory

<sup>3</sup> Shanghai Jiao Tong University <sup>4</sup> Monash University

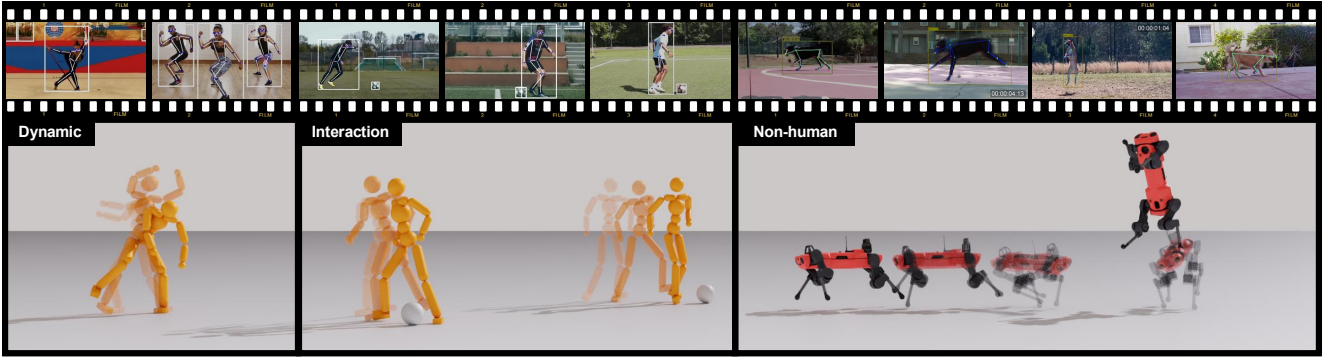


Figure 1. The proposed **Mimic2DM** effectively learns character controllers for diverse motion types, including dynamic human dancing, complex ball interactions, and agile animal movements, by directly imitating 2D motion sequences extracted from in-the-wild videos.

## Abstract

Video data is more cost-effective than motion capture data for learning 3D character motion controllers, yet synthesizing realistic and diverse behaviors directly from videos remains challenging. Previous approaches typically rely on off-the-shelf motion reconstruction techniques to obtain 3D trajectories for physics-based imitation. These reconstruction methods struggle with generalizability, as they either require 3D training data (potentially scarce) or fail to produce physically plausible poses, hindering their application to challenging scenarios like human-object interaction (HOI) or non-human characters. We tackle this challenge by introducing **Mimic2DM**, a novel motion imitation framework that learns the control policy directly and solely from widely available 2D keypoint trajectories extracted from videos. By minimizing the reprojection error, we train a general single-view 2D motion tracking policy capable of following arbitrary 2D reference motions in physics simulation, using only 2D motion data. The policy, when trained on diverse 2D motions captured from different or slightly different viewpoints, can further acquire

3D motion tracking capabilities by aggregating multiple views. Moreover, we develop a transformer-based autoregressive 2D motion generator and integrate it into a hierarchical control framework, where the generator produces high-quality 2D reference trajectories to guide the tracking policy. We show that the proposed approach is versatile and can effectively learn to synthesize physically plausible and diverse motions across a range of domains, including dancing, soccer dribbling, and animal movements, without any reliance on explicit 3D motion data. **Project Website:** <https://jiann-li.github.io/mimic2dm/>

## 1. Introduction

Controlling physically simulated characters to perform realistic motion and plausible object interactions remains a fundamental yet challenging problem in computer animation and robotics. Recently, motion imitation techniques have leveraged motion capture (MoCap) data to train physics-based character controllers, achieving impressive results in producing highly dynamic and physically realistic motions on the simulated virtual character [7, 12, 13, 29, 35, 52].

However, collecting high-quality 3D MoCap data is costly and labor-intensive, as it requires numerous skilled performers and specialized capture systems.

To address the scarcity of high-quality MoCap 3D data, recent studies have explored exploiting videos as an alternative data source. Most existing methods [24, 30, 59, 62] leverage off-the-shelf human motion reconstruction techniques to estimate 3D motions from videos for learning physics-based skills. While advanced training-based estimation methods can achieve remarkable accuracy and realism in reconstructing human motions, their performance heavily depends on extensive high-quality 3D data for training, limiting their applicability in domains with scarce 3D data, such as human-object interactions or non-human motions. Moreover, these methods often result in physically implausible motions due to a lack of physics constraints, which in turn hinders subsequent motion imitation.

In contrast to training on unreliable 3D motions estimated from videos, some studies have demonstrated the possibility of directly utilizing 2D motions extracted from the video footage as supervision, achieving success across various 3D tasks [3, 11, 16, 33, 44]. This 2D data is highly accessible and can be easily extracted from videos for a wide range of skeletons, including object interactions and non-human (animal) movements. Additionally, 2D keypoint motion detected in videos provides unbiased 2D evidence that accurately reflects the original movements present in the footage. The key challenge when employing 2D data is the missing depth information. While 2D priors combined with geometrical constraints can yield visually plausible 3D poses, the resulting motions are often physically limited and cannot be directly utilized as high-quality data for motion imitation.

In this paper, we present Mimic2DM, a generic imitation learning framework capable of acquiring a wide range of complex, physics-based skills, including human-object interaction (HOI) and animal locomotion, by relying solely on widely available 2D motion data extracted from videos. To leverage 2D motion data, we formulate a physics-based 2D motion tracking by unifying 3D reconstruction and physics-based motion imitation into a single reprojection minimization task, which is optimized via reinforcement learning (RL). With the inclusion of physical constraints, the learned policy is able to synthesize physically correct 3D motions by directly imitating from the depth-absent 2D data. Building on this, we introduce a view-agnostic tracking policy. This design not only allows the policy to benefit from diverse viewpoints in the data, thereby learning more realistic 3D motions, but also facilitates easy extension to a multi-view tracking policy for general 3D motion tracking tasks. To enhance training efficiency for single-view motion tracking, we propose an adaptive state initialization strategy along with a reprojection-error-based early termination

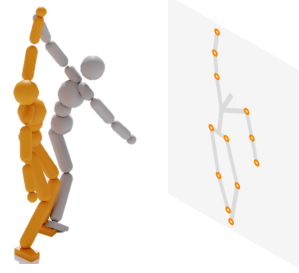


Figure 2. **Ambiguity caused by 3D-to-2D gap.** When given the 2D tracking controller with only single-view 2D motion as inputs, controllers might struggle to achieve different poses, as illustrated in the figure, the orange colored character and the grey colored character both achieve minimized reprojection error for the given 2D reference.

criterion. Finally, to extend this framework for generative tasks such as novel motion synthesis, we employ a hierarchical control structure that integrates the tracking policy with a 2D motion generator, where 2D motions serve as an interface between the motion generator and the control policy.

We demonstrate that Mimic2DM can effectively learn a range of challenging physical skills like skillful soccer ball interaction and highly dynamic movements in a robotic dog, using only 2D motion sequences extracted from in-the-wild videos. We further demonstrate that the proposed view-agnostic 2D tracking policy exhibits universal tracking capabilities. As casual videos are likely to be acquired from different or slightly different viewpoints, the single-view policy trained on this data can be effectively extended to a multi-view tracking policy via a view-aggregation mechanism, enabling it to perform 3D tracking. Crucially, we show that, even trained exclusively on 2D data, our approach achieves comparable 3D tracking accuracy to that of 3D motion-trained conventional methods. Furthermore, we highlight the generative potential of our approach by extending it into a hierarchical framework with a 2D motion generator for motion synthesis and conditional control. In this setup, we demonstrate that our proposed autoregressive 2D motion generator surpasses current diffusion-based models in producing the high-quality 2D motion sequences required to effectively guide the tracking policy.

## 2. Related Works

### 2.1. Physics-based Character Control

Achieving realistic and physically plausible character behaviors is a key goal and challenge in computer animation. To this end, physics simulation is employed to emulate the complex motion dynamics and collision interactions of virtual characters. In early works, physics-based character animation principally focused on locomotion behaviors using

traditional optimization-based control strategies combined with some heuristic rules [4, 5, 8, 34, 57, 58]. Subsequently, reinforcement learning (RL) was introduced to enable simulated characters to master a wide range of complex skills ranging from basic locomotive skills [27, 28, 36, 38] to proficient sports skills [2, 18]. However, designing effective reward functions typically necessitates specialized knowledge, and the behaviors generated by reinforcement learning controllers often exhibit irregular motion patterns. To address these issues, MoCap data is employed to train physically simulated character controllers. This can be achieved through explicit motion tracking rewards [1, 14, 19, 26, 29] or by utilizing implicit motion style rewards derived from a discriminator [7, 31, 49]. These approaches enable the learning of more natural and coherent character behaviors.

To re-purpose the learned skills for a wide range of downstream tasks, recent work has explored using latent-based generative models, such as VAEs [20, 47, 54, 55] and GANs [6, 9, 10, 32, 39], to learn reusable motion primitives by mapping motion clips into a low-dimensional latent space. These approaches can efficiently learn a separate high-level policy that controls the pre-trained latent-represented skills for each downstream task. Another line of work focuses on the combination of a universal motion tracking controller with kinematic motion generative models [15, 40, 51]. This hierarchical control framework also supports versatile, physically plausible motion synthesis and control [37, 41, 48, 52]. However, all of these approaches rely on high-quality 3D MoCap data for training, significantly restricting their applicability and scalability. In contrast, our method is a motion imitation approach that only requires 2D motion data, making it more accessible and versatile.

## 2.2. Learning Physically Skills from Videos

Compared to motion capture (MoCap) data, videos are a more accessible source for learning physics-based skills. Early work by Vondrak et al. [43] attempted to reproduce jumping and gymnastic motions in a physics-simulated environment by minimizing silhouette loss from monocular videos. Recent advances in computer vision have enabled the reconstruction of 3D human poses from videos, which can be leveraged to train physics-based character controllers. Initial attempts focused on reproducing individual motion instances in a physics simulator derived from single videos. For example, Peng et al. [30] proposed a motion imitation pipeline that tracks 3D poses estimated from video. Building on this, Yu et al. [59] advanced the technique by incorporating additional cues such as 2D/3D poses and foot contacts into policy learning, enabling the synthesis of agile motions from long video sequences with dynamic camera movements. To avoid time-consuming physics-based motion imitation for new video

clips, Yuan et al. [61] introduced a real-time physically motion estimation approach SimPoe. SimPoe employs a universal physics-based tracking controller trained on a large-scale 3D motion dataset AMASS [21] as the motion corrector. Recently, video data has demonstrated its superior accessibility and scalability for learning intricate skills that are difficult or costly to capture in a laboratory environment [24, 45, 46, 50, 62]. However, a major challenge is that 3D poses from video are not physically reliable. This data therefore requires extensive post-processing or even manual correction before it can be used to train a physics-based control policy. In contrast, our method performs end-to-end learning directly from 2D pose sequences, making it applicable to 'in-the-wild' videos and adaptable to various character skeletons.

## 3. Method

### 3.1. Imitation as Reprojection Minimization

Given a 2D motion sequence denoted by as a series of coordinates  $\mathbf{X} \in \mathbb{R}^{T \times J \times 2}$ , where  $T$  is the motion length and  $J$  is the number of keypoints (including skeleton joints or object landmarks), our goal is to learn a policy  $\pi$  capable of controlling the simulated character to perform physically plausible 3D motions such that their 2D projection onto a given camera view aligns precisely with the provided 2D motion reference. Existing approaches often separately reconstruct 3D motion from the 2D evidence and learn a control policy to imitate the reconstructed 3D motion. Due to the ill-posed nature of 2D-to-3D inversion, the reconstructed 3D motions are often physically infeasible, especially in domains such as object interaction or non-human locomotion where 3D priors are unavailable. This flawed 3D supervision poses a major obstacle to motion imitation and often leads to the failure of learning. To address this, we propose to unify motion reconstruction and motion imitation by formulating a physics-based 2D motion tracking problem defined by the following:

$$\min_{\pi} \mathbb{E}_{s_0 \sim d(s_0)} \|P_{\pi}(C) - \mathbf{X}\| \quad \text{s.t.} \quad f_{\pi} = 0, \quad (1)$$

where  $P_{\pi}(C)$  denotes the 2D projection of the 3D joint positions synthesized by the policy  $\pi$  under the camera view  $C$ ,  $d(s_0)$  is the distribution of the initial state, and  $f_{\pi} = 0$  represents the physical constraints and underlying MDP dynamics of the simulated character. The unified formulation allows for end-to-end error minimization and leverages physics constraints to regularize the resultant 3D motions, thereby ensuring physical plausibility.

### 3.2. View-agnostic 2D Tracking Policy

Optimizing solely for the reprojection objective is inherently limited by depth ambiguity, often leading to implausible or unnatural poses. To mitigate this issue, we observe

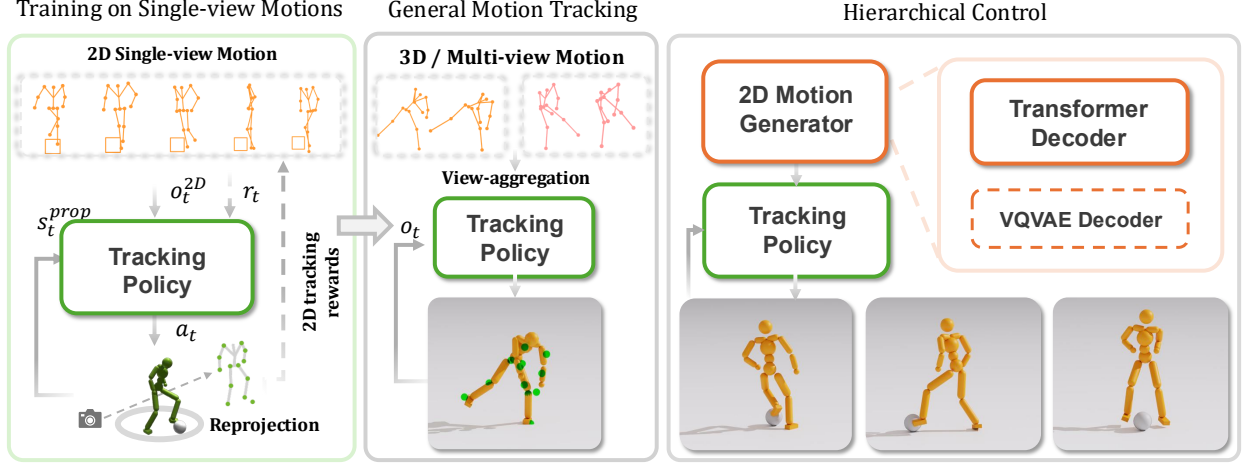


Figure 3. **Overview of the pipeline.** Our approach Mimic2DM learns a view-agnostic tracking policy that imitates 2D motion sequences extracted from videos. The resulting policy can be zero-shot adapted to multi-view tracking via view aggregation, and integrated with a 2D motion generator for generative tasks.

that casual videos are typically captured from a variety of viewpoints, which collectively provide sufficient information to depict the motion. Building on this insight, we propose training a general 2D tracking policy designed to minimize the reprojection error for a given reference motion under arbitrary camera viewpoints. Such a policy implicitly acquires a 3D understanding of motion, as it learns to satisfy 2D reprojection constraints from diverse viewing directions present in the data. Furthermore, this cross-view generalization capability enables the policy to be effectively extended to multi-view motion tracking via feature aggregation, thereby achieving robust 3D motion tracking performance without relying on any 3D supervision.

The 2D tracking policy is represented as a neural network that receives inputs of the character’s proprioceptive  $s_t^{\text{prop}}$  [29] and the observation of future 2D motion reference  $\mathbf{o}_t^{2D}$ , then predicts the simulated character’s PD (Proportional-Derivative) targets as a diagonal Gaussian distribution over the action space.

**View-agnostic 2D Observations** To achieve better generalization ability for arbitrary-view 2D motion tracking, we intentionally omit any explicit camera view information from the observations, thereby compelling the policy to infer the viewpoint of the 2D motion reference solely from the character’s actual 2D projection within the simulation.

The proposed 2D observation is represented by:

$$\mathbf{o}_t^{2D|C} = [P(\mathbf{x}_t^{3D}, C), \mathbf{x}_{t:t+L}], \quad (2)$$

where  $\mathbf{x}_{t:t+L} \in \mathbb{R}^{L \times J \times 2}$  is the clip of future 2D reference motion, looking ahead over  $L$  frames, and  $P(\mathbf{x}_t^{3D}, C) \in \mathbb{R}^{J \times 2}$  denotes the 2D projection of the 3D keypoints  $\mathbf{x}_t^{3D} \in \mathbb{R}^{J \times 3}$  in simulation.

**View Aggregation for 3D Motion Tracking** The diverse-view data provides a well-constrained motion space, thereby leading to more physically plausible 3D motions synthesized by the view-agnostic tracking policy. However, the inherent ambiguity of a single 2D projection still persists, which limits the policy’s fine-grained controllability in 3D space. As shown in Figure 3, we propose to adapt our policy to a multi-view tracking policy by introducing a view-aggregation technique to mitigate this issue.

We first demonstrate how to extend the capabilities of the general 2D single-view tracking policy to achieve 3D motion tracking by reframing the single-view objective into a multi-view setup. We define a multi-view tracking problem by considering  $K$  multi-view 2D motions and their corresponding camera views,  $\{\mathbf{X}_k, C_k\}_{k=1}^K$ , which are all projected from a single underlying 3D motion sequence. The objective to find a policy  $\pi$  that minimizes the aggregate reprojection error across all views is

$$\min_{\pi} \mathbb{E}_{s_0 \sim d(s_0)} \sum_{k=1}^K \|P_{\pi}(C_k) - \mathbf{X}_k\| \quad \text{s.t.} \quad f_{\pi} = 0. \quad (3)$$

We hypothesize that the optimality attained by the general single-view tracking policy is sufficient to achieve optimality for the multi-view tracking problem defined above.

To enable the policy to accept 2D observations from multiple views  $\{\mathbf{o}_t^{2D|C_1}, \mathbf{o}_t^{2D|C_2}, \dots, \mathbf{o}_t^{2D|C_K}\}$ , we devised a view aggregation strategy for combining information across different views. Leveraging the linearity typically observed in the neural network feature space, we opt to average the feature embeddings of the 2D observations from all views. The multi-view motion tracking policy  $\pi_{\text{mv}}$  adapted from



the view-agnostic tracking controller is defined as:

$$\pi_{\text{mv}}(a_t | \mathbf{s}_t^{\text{prop}}, \mathbf{o}_t^{2\text{D}|C_1}, \dots, \mathbf{o}_t^{2\text{D}|C_K}) = \pi(a_t | \mathbf{s}_t^{\text{prop}}, \mathbf{o}_t^{\text{agg}}), \quad (4)$$

where the aggregated feature  $\mathbf{o}_t^{\text{agg}}$  is computed by averaging the view-specific features:

$$\mathbf{o}_t^{\text{agg}} = \frac{1}{N} \sum_{i=1}^N \phi(\mathbf{o}_t^{2\text{D}_i}), \quad (5)$$

where  $\phi(\cdot)$  denotes the feature extractor for single-view 2D observations. The proposed view-aggregation strategy grants the view-agnostic tracking policy the capability for multi-view motion tracking without requiring any fine-tuning, thereby greatly enhancing its 3D controllability.

### 3.3. Training for Single-view Tracking

Training the view-agnostic 2D tracking policy follows a similar reinforcement learning paradigm to 3D motion tracking, with three key adaptations: 2D tracking rewards specifically designed to minimize the reprojection error, an adaptive state-initialization to resolve the lack of high-quality 3D reference poses, and an early termination strategy tailored for 2D motion imitation training.

**2D Tracking Rewards** To encourage the minimization of reprojection error in Eq. 1, we employ a distance-based reward function as the 2D tracking reward, combined with an energy consumption penalty for regularization  $r_t = w_p r_t^p + w_e r_t^e$ , where  $w_p$  and  $w_e$  are reward weights. The 2D tracking reward  $r_t^p$  is computed by measuring the discrepancy between the projected 2D keypoints and the reference 2D points:

$$r_t^p = \exp \left( -\alpha \sum_{j=1}^J \|P(\mathbf{x}_t^{3\text{D}|j}) - \mathbf{x}_t^j\| \right), \quad (6)$$

where  $\mathbf{x}_t^j$  denotes the coordinates of the  $j$ -th reference keypoint at time  $t$ ,  $P(\mathbf{x}_t^{3\text{D}|j})$  denotes the projected 2D coordinates of the simulated character joint, and  $\alpha$  is a positive scalar. The energy consumption penalty  $r_t^e$  is computed as  $r_t^e = -\sum_j \|\dot{\mathbf{q}}_t^j \cdot \tau_t^j\|$ , where  $\dot{\mathbf{q}}_t^j$  and  $\tau_t^j$  denote the joint velocity and torque for joint  $j$  at time  $t$ , respectively.

**Adaptive State Initialization** The distribution of initial states is crucial for learning efficiency of RL. In conventional 3D motion imitation, the widely adopted Reference State Initialization (RSI) [29] relies on accurate 3D motion states, which are unavailable when only 2D data is provided. Although imperfect 3D reconstructions [60, 61] or manually specified default poses can be utilized for state initialization, the occurrence of physically infeasible states will

significantly impede the policy learning. To address this limitation, we propose to discard suboptimal initial states by evaluating the estimated tracking performance using the critic network. Inspired by the approach in [30], which learns a neural network policy to predict a distribution of initial states, we instead employ a data buffer to maintain a discrete representation of the initial state distribution for enhanced training stability.

Specifically, a dedicated buffer is maintained for each reference frame and is initially populated with arbitrary initial 3D poses. During training, states obtained from policy rollouts are evaluated using the critic network, and those states that achieve a high critic score are subsequently stored in the corresponding frame buffer. To facilitate prioritized exploration, the sampling probability for each stored state is set to be exponentially proportional to its score.

**Reprojection-based Early Termination** To ensure training efficiency and avoid unrecoverable states of the simulated character, we introduce an early termination mechanism based on the reprojection error. Specifically, an episode is terminated when the character’s projected pose deviates significantly from the reference 2D pose.

### 3.4. Hierarchical Control via 2D Interface

The trained view-agnostic 2D tracking policy can be extended to generative tasks via integration with a kinematic 2D motion generative model, forming a hierarchical controller. To enable real-time, infinite-length motion synthesis, we propose a transformer-based autoregressive 2D motion generator. This GPT-like architecture ensures on-the-fly generation while preserving high-quality motion characteristics. To efficiently encode the global movements in 2D motion, we introduce a canonical 2D motion representation, facilitating the learning of our 2D motion generator.

**Canonical Representation of 2D Motion** Raw 2D keypoint coordinates often exhibit significant variance due to global character movement, such as lateral displacement (e.g., moving from right to left) or changes in scale caused by translation along the camera axis (e.g., moving closer to or farther from the camera). This high variance makes training the generative model challenging. To mitigate this problem, we propose a canonicalized 2D motion representation that is more efficient for neural network learning while still preserving the necessary global motion information.

More specifically, we compute the root translation  $x^{\text{root}}$ , a scale factor  $s$ , and the local pose  $\bar{x}$  using the formulation  $\bar{x} = (x - x^{\text{root}})/s$  for each frame. The relative scale change between consecutive frames is given by  $\delta s_t = \log(s_t/s_{t-1})$ , while the normalized shift in root translation is defined as  $\delta x_t^{\text{root}} = (x_t^{\text{root}} - x_{t-1}^{\text{root}})/s_t$ . The relative 2D motion sequence is then represented as  $\mathbf{x}^{\text{can}} =$

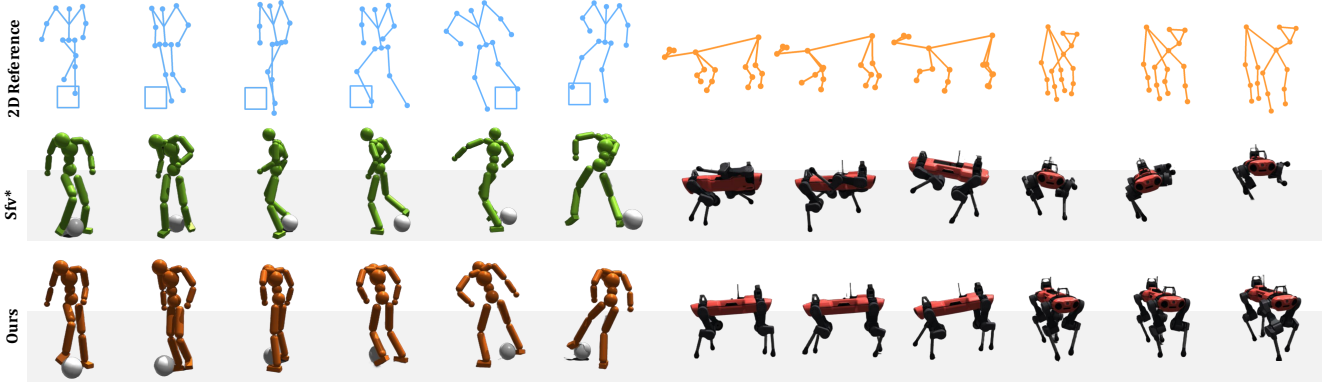


Figure 4. **Qualitative comparison** between our method (bottom) and the adapted Sfv\* [30] (middle) on imitating 2D reference motions (top) from Soccer Dribble and Animal. Sfv\* struggles to reproduce complex ball-foot interactions (left) and often yields unnatural motions (right) due to inaccuracies in the reconstructed 3D training data. Sfv\* is adapted to learn from 3D motions reconstructed via reprojection loss minimization.

$[x_0^{\text{can}}, x_1^{\text{can}}, \dots, x_T^{\text{can}}]$ , where each  $x_t^{\text{can}} = (\bar{x}_t, \delta x_t^{\text{root}}, \delta s_t)$ . Given the scale and root translation of the initial frame,  $x_0^{\text{root}}$  and  $s_0$ , we can convert between the absolute and relative 2D motion representations. The forward and inverse transformations are defined as:

$$\mathbf{X}^{\text{can}} = G(\mathbf{X}), \quad \mathbf{X} = G^{-1}(\mathbf{X}^{\text{can}}, x_0^{\text{root}}, s_0). \quad (7)$$

**2D Motion Tokenizer** We employ a Vector-Quantized Variational Autoencoder (VQ-VAE) [42] to compress redundant information and discretize the canonical 2D motion sequence into a sequence of compact tokens. To maintain accurate global translation and scale consistency over long sequences, we introduce an additional absolute 2D reconstruction term into the loss function, computed by transforming the canonical representation back to the global coordinate space:

$$\mathcal{L}_{\text{rec}} = \|\mathbf{X}^{\text{can}} - \hat{\mathbf{X}}^{\text{can}}\| + \omega \|G^{-1}(\mathbf{X}^{\text{can}}) - G^{-1}(\hat{\mathbf{X}}^{\text{can}})\|, \quad (8)$$

where  $\omega$  is a weighting factor for the absolute loss term, and  $\hat{\mathbf{X}}^{\text{can}}$  denotes reconstructed canonical 2D motion by the VQ-VAE. Furthermore, to achieve autoregressive token detokenization, we adopt causal convolutional layers [25] in the VQ-VAE architecture.

**Autoregressive Generator** By tokenizing the 2D motion sequence into discrete codebook indices using VQ-VAE,  $\mathbf{c} = [c_0, c_1, \dots, c_{T/l}]$ , the data distribution is modeled as a discrete, factorized distribution:  $p(\mathbf{c}) = \prod_{i=1}^{T/l} p(c_i | c_0, \dots, c_{i-1})$  where  $c_i \in \{1, \dots, K\}$ . We employ a causal transformer to represent this distribution, denoted as  $p_{2D}(c_0, c_1, \dots, c_{T/l} | y)$ , where  $y$  is an optional conditioning variable (with  $y = \emptyset$  for unconditional generation). The model is trained by minimizing the cross-entropy loss between the target token index and the predicted probability.

Method	Soccer Dribble				Animal		
	Succ. <sup>↑</sup>	$E_{2D}$ <sup>↓</sup>	$E_{O2D}$ <sup>↓</sup>	Jitters <sup>↓</sup>	Succ. <sup>↑</sup>	$E_{2D}$ <sup>↓</sup>	Jitters <sup>↓</sup>
Sfv* [30]	47.8	19.9	38.2	2.62	50.0	68.9	9.20
Ours	<b>91.3</b>	<b>17.1</b>	<b>17.5</b>	<b>1.69</b>	<b>83.3</b>	<b>26.8</b>	<b>3.36</b>

Table 1. **Quantitative comparison** of our method against the two-stage pipeline Sfv\* [30] on our collected Soccer Dribble and Animal datasets sourced from in-the-wild videos. Sfv\* is adapted to learn from 3D motions reconstructed via reprojection loss minimization.

**Interface for Hierarchical Control** The trained view-agnostic 2D motion tracking policy can be integrated with our 2D motion generators, forming a hierarchical controller capable of a wide range of generative tasks. The generated  $L$  2D motion reference frames  $\hat{\mathbf{x}}_{t:t+L}^{\text{can}}$ , are first converted to the global representation via  $\hat{\mathbf{x}}_{t:t+L} = G^{-1}(\hat{\mathbf{x}}_{t:t+L}^{\text{can}})$ . We regard the generated 2D motions in the global coordinate as the reference motion for our tracking policy. Benefiting from our view-agnostic training, the viewpoint used for projection can be arbitrarily selected. This design eliminates rigid constraints on viewpoints, enhancing the controller’s applicability across diverse scenarios.

## 4. Experiments

### 4.1. Experimental Setup

**Data** We evaluate the effectiveness of our framework using both in-the-wild videos and public datasets. To assess its ability to learn from challenging scenarios with scarce 3D data, such as HOI and non-human motions, we curate two new datasets of soccer dribbling and animal motions. **Soccer Dribble** is collected from online videos showcasing a diverse range of complex soccer dribbling skills that involve intricate football interaction dynamics. We apply

Training Data	Inputs	AIST++ [17]-Train				AIST++ [17]-Test				2D Motion Generator			
		Succ. <sup>↑</sup>	$E_{3D}$ <sup>↓</sup>	$E_{2D}$ <sup>↓</sup>	Jitters <sup>↓</sup>	Succ. <sup>↑</sup>	$E_{3D}$ <sup>↓</sup>	$E_{2D}$ <sup>↓</sup>	Jitters <sup>↓</sup>	Succ. <sup>↑</sup>	$E_{2D}$ <sup>↓</sup>	FID <sup>↓</sup>	Jitters <sup>↓</sup>
3D	3D	92.1	114.5	18.9	2.81	89	141	21.3	2.99	-	-	-	-
2D	1-view 2D	88.4	220.0	35.1	1.64	82.5	254.6	38.6	1.79	86.9	42.1	1.52	2.08
	2-view 2D	90.1	147.8	22.1	1.58	88.0	164.9	24.5	1.60	92.1	28.9	2.44	2.07
	3-view 2D	90.4	144.3	21.9	1.58	88.9	161.5	24.1	1.60	88.6	33.1	2.84	1.90

Table 2. **Quantitative evaluation** of large-scale motion imitation on AIST++ [17] and on 2D motions generated by our autoregressive 2D motion generator. Our approach achieves performance comparable to baselines trained on ground-truth 3D data.



Figure 5. **Visualization of synthesized ball-dribbling motions** using our hierarchical controller. Our framework learns diverse skills from 2D motion data, exhibits natural transitions between different dribbling styles (left), and demonstrates seamless composition and switching between directional movements.

Motion	Method	FID <sup>↓</sup>	Succ. <sup>↑</sup>	Jitters <sup>↓</sup>
Soccer Dribble	Diffusion	6.29	0.13	2.16
	AR (Ours)	<b>5.16</b>	<b>0.71</b>	<b>1.91</b>
AIST++	Diffusion	5.92	0.44	<b>1.87</b>
	AR (Ours)	<b>2.44</b>	<b>0.92</b>	2.07

Table 3. **Comparative evaluation of generative models** within the hierarchical control framework on the Soccer Dribble and AIST++ datasets.

ViTPose [53] to detect and extract 2D human poses and ball bounding boxes from these videos. **Animal** is also sourced from online videos and includes various dog movements such as walking, running, and jumping. The 2D key-points are detected and processed using the same pipeline as the Dribble dataset. For benchmarking, we also include the **AIST++** dataset [17], a large-scale public dataset containing dynamic dance videos captured from multiple view-points with annotated 3D human poses. Following the protocol in [16], we generate a single-view 2D motion data by randomly selecting a single camera view per sequence.

**Metrics** We adopt the following metrics for quantitative evaluation. *Success Rate* measures the robustness of the control policy and is defined as the percentage of successfully tracked motions over all reference motions. A trial is considered unsuccessful if the maximum reprojection error exceeds 100 pixels. *2D Tracking Error* evaluates the policy’s tracking accuracy in 2D space and is computed as the average reprojection error between the character’s projected poses and the reference motion. *2D Object Tracking*

*Error* is similarly defined but measures the accuracy of object tracking in human–object interaction (HOI) tasks. *3D Tracking Error* assesses the tracking accuracy with respect to 3D reference motions by averaging the positional joint errors across all frames. *Jitters* quantifies the physical plausibility of the synthesized motion by computing the third-order derivatives of joint positions as a measure of motion smoothness. Finally, *FID* measures the distributional difference between the synthesized and reference motions. Following the protocol in [11], FID scores are computed on the 2D projections of the synthesized poses.

**Implementation Details** The control policy is running at 30Hz and interacts with the physics simulator Isaac Gym [23], which simulates dynamics at 60Hz. The control policy is an MLP network with 512, 256, 256 hidden units. For the Vector-Quantized Variational Autoencoder (VQ-VAE), we set the codebook size to 512 with an embedding dimension of 128. The autoregressive transformer employs a decoder architecture with four layers, four attention heads, and an embedding dimension of 128. We simply optimize the reprojection loss obtain the initial poses as initial states for single-view tracking training. Note that our approach is not sensitive to the initial states, we can obtain them through various methods, including state-of-the-art pose estimation techniques or manual specification. The training of the single-view tracking policy takes approximately one week for both AIST++ motions and Dribble motions, using four NVIDIA P40 GPUs. The imitation of animal motions takes about three days with the same resources.

## 4.2. Evaluation on Motion Imitation

**Comparison with Two-stage Approach** We evaluate our approach on the challenging HOI and non-human motion datasets (Soccer Dribble and Animal). We also conduct a detailed comparison against the typical two-stage baseline, Sfv [30], which first estimates 3D poses before imitating with the reconstructed trajectories. Since the original Sfv [30] was not designed for domains like HOI or animal motions, we adapted its motion reconstruction stage for a fair comparison. For the Soccer Dribble dataset, we utilized SLAHMR [56] to obtain the 3D human poses. The ball’s 3D position was subsequently reconstructed by minimizing the reprojection loss on its bounding box and incorporating the estimated depth of the ball. For the Animal motion data, we simply solve an inverse kinematics problem by optimizing the reprojection loss since there is no data prior available.

The quantitative comparison results, presented in Table 1, demonstrate the superior performance of our approach against the baseline. Our method achieves both a higher learning success rate and lower motion jitters and with lower 2D tracking error and object 2D tracking error. The qualitative comparison (Figure 4) illustrates the limitation of the baseline: Sfv\* fails to learn complex ball turnaround interactions and exhibits implausible quadruped locomotion due to imperfect training motions. In contrast, our approach successfully synthesizes realistic motions that accurately align with the 2D references.

**General Motion Tracking** The view-agnostic tracking policy is generalizable and can achieve zero-shot multi-view motion tracking via view-aggregation. To thoroughly evaluate its tracking ability, we train our approach on the AIST++ dataset and compare it with the 3D motion imitation baseline trained using ground-truth 3D motions.

As shown in Table 2, the trained single-view tracking policy successfully generalizes to unseen test and generated motions. Furthermore, the proposed view-aggregation mechanism grants the policy multi-view tracking capability, boosting 3D motion understanding with lower 3D motion tracking error, and even achieving performance comparable to the 3D baseline trained on ground-truth data.

## 4.3. Evaluation on Hierarchical Control

To evaluate the effectiveness of our hierarchical control framework using 2D motion interfaces, we train the 2D motion generator on the AIST++ and Soccer Dribble datasets. Qualitatively, the trained motion generator successfully demonstrates the ability to synthesize complex trajectories by seamlessly combining different motion skills, as illustrated by the transition between various dribbling skills in Figure 5. We further benchmarked our proposed autoregressive (AR) 2D motion generator against the diffusion-based model baseline [41]. As detailed in Table 3, our AR gen-

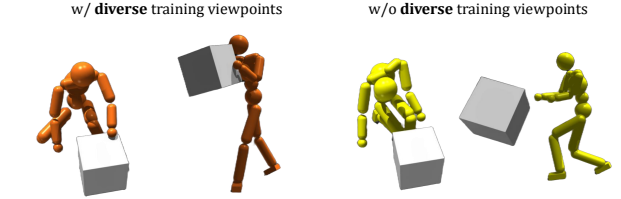


Figure 6. **Exploiting viewpoint diversity in the data.** Our view-agnostic tracking policy learns a stronger 3D understanding of character poses when trained on diverse viewpoints (left). In contrast, a policy trained on homogeneous viewpoints exhibits unnatural behaviors and fails to acquire interaction skills (right).

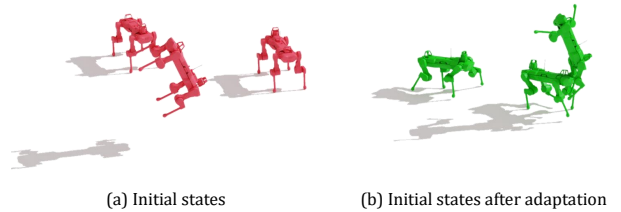


Figure 7. **Effectiveness of adaptive state initialization.** Our method adaptively updates and refines physically implausible initial states (left) into more feasible ones (right), enabling more efficient policy training.

erator demonstrates superior performance in synthesizing more realistic 2D guidance, achieving a lower FID score and higher success rate compared to the baseline.

## 4.4. Ablation Study

**View Diversity in Dataset** To investigate how effectively our approach benefits from the diversity of viewpoints in the training data, we conducted an ablation study. We trained two variants of the policy: one using 2D motions projected from the same 3D instance with diverse viewpoints, and a second using 2D motions with homogeneous viewpoints. As illustrated in Figure 6, the policy trained on diverse-view motions synthesizes significantly more natural-looking behavior than that trained solely on homogeneous-view motions. Notably, the homogeneous-view policy failed to execute the challenging “lift the box” interaction, underscoring the importance of view diversity for learning complex skills.

**Adaptive State Initialization** We evaluate the effectiveness of our proposed adaptive state initialization strategy for single-view tracking training. As shown in Figure 7, the adaptive state initialization can significantly update the initial states from the erroneous initialization.

## 5. Conclusion

In this work, we present a novel approach to leveraging video data for learning physics-based character controllers by training a view-agnostic tracking policy to directly imitate 2D motion sequences extracted from videos. Our



framework generalizes robustly across diverse motions and character articulations, successfully learning complex HOI motions and agile non-human movements without access to any 3D motion data. Furthermore, by incorporating view aggregation, our trained policy achieves 3D tracking performance comparable to baselines trained directly on ground-truth 3D data. Finally, by integrating the policy with a proposed autoregressive 2D motion generator, we establish a hierarchical controller capable of generating physically plausible motions, demonstrating significant potential for a variety of downstream tasks.

## References

- [1] Kevin Bergamin, Simon Clavet, Daniel Holden, and James Richard Forbes. Drecon: data-driven responsive control of physics-based characters. *ACM Transactions On Graphics (TOG)*, 38(6):1–11, 2019. 3
- [2] Jason Chemin and Jehee Lee. A physics-based juggling simulation using reinforcement learning. In *Proceedings of the 11th ACM SIGGRAPH Conference on Motion, Interaction and Games*, pages 1–7, 2018. 3
- [3] Ching-Hang Chen, Ambrish Tyagi, Amit Agrawal, Dylan Drover, Rohith Mv, Stefan Stojanov, and James M Rehg. Unsupervised 3d pose estimation with geometric self-supervision. In *Proceedings of the IEEE/CVF conference on computer vision and pattern recognition*, pages 5714–5724, 2019. 2
- [4] Stelian Coros, Philippe Beaudoin, and Michiel Van de Panne. Generalized biped walking control. *ACM Transactions On Graphics (TOG)*, 29(4):1–9, 2010. 3
- [5] Martin De Lasa, Igor Mordatch, and Aaron Hertzmann. Feature-based locomotion controllers. *ACM transactions on graphics (TOG)*, 29(4):1–10, 2010. 3
- [6] Zhiyang Dou, Xuelin Chen, Qingnan Fan, Taku Komura, and Wenping Wang. C-ase: Learning conditional adversarial skill embeddings for physics-based characters. In *SIGGRAPH Asia 2023 Conference Papers*, pages 1–11, 2023. 3
- [7] Mohamed Hassan, Yunrong Guo, Tingwu Wang, Michael Black, Sanja Fidler, and Xue Bin Peng. Synthesizing physical character-scene interactions. In *ACM SIGGRAPH 2023 Conference Proceedings*, pages 1–9, 2023. 1, 3
- [8] Jessica K Hodgins, Wayne L Wooten, David C Brogan, and James F O’Brien. Animating human athletics. In *Proceedings of the 22nd annual conference on Computer graphics and interactive techniques*, pages 71–78, 1995. 3
- [9] Jordan Juravsky, Yunrong Guo, Sanja Fidler, and Xue Bin Peng. Padl: Language-directed physics-based character control. In *SIGGRAPH Asia 2022 Conference Papers*, pages 1–9, 2022. 3
- [10] Jordan Juravsky, Yunrong Guo, Sanja Fidler, and Xue Bin Peng. Superpadl: Scaling language-directed physics-based control with progressive supervised distillation. In *ACM SIGGRAPH 2024 Conference Papers*, pages 1–11, 2024. 3
- [11] Roy Kapon, Guy Tevet, Daniel Cohen-Or, and Amit H Bermano. Mas: Multi-view ancestral sampling for 3d motion generation using 2d diffusion. In *Proceedings of the IEEE/CVF Conference on Computer Vision and Pattern Recognition*, pages 1965–1974, 2024. 2, 7
- [12] Seyoung Lee, Sunmin Lee, Yongwoo Lee, and Jehee Lee. Learning a family of motor skills from a single motion clip. *ACM Transactions on Graphics (TOG)*, 40(4):1–13, 2021. 1
- [13] Seunghwan Lee, Phil Sik Chang, and Jehee Lee. Deep compliant control. In *ACM SIGGRAPH 2022 conference proceedings*, pages 1–9, 2022. 1
- [14] Yoonsang Lee, Sungeun Kim, and Jehee Lee. Data-driven biped control. In *ACM SIGGRAPH 2010 Papers*, New York, NY, USA, 2010. Association for Computing Machinery. 3
- [15] Jiaman Li, Jiajun Wu, and C Karen Liu. Object motion guided human motion synthesis. *ACM Transactions on Graphics (TOG)*, 42(6):1–11, 2023. 3
- [16] Jiaman Li, C Karen Liu, and Jiajun Wu. Lifting motion to the 3d world via 2d diffusion. *arXiv preprint arXiv:2411.18808*, 2024. 2, 7
- [17] Ruilong Li, Shan Yang, David A Ross, and Angjoo Kanazawa. Ai choreographer: Music conditioned 3d dance generation with aist++. In *Proceedings of the IEEE/CVF international conference on computer vision*, pages 13401–13412, 2021. 7
- [18] Libin Liu and Jessica Hodgins. Learning basketball dribbling skills using trajectory optimization and deep reinforcement learning. *ACM Transactions on Graphics (TOG)*, 37(4):1–14, 2018. 3
- [19] Zhengyi Luo, Jinkun Cao, Kris Kitani, Weipeng Xu, et al. Perpetual humanoid control for real-time simulated avatars. In *Proceedings of the IEEE/CVF International Conference on Computer Vision*, pages 10895–10904, 2023. 3
- [20] Zhengyi Luo, Jinkun Cao, Josh Merel, Alexander Winkler, Jing Huang, Kris M Kitani, and Weipeng Xu. Universal humanoid motion representations for physics-based control. In *The Twelfth International Conference on Learning Representations*, 2023. 3
- [21] Naureen Mahmood, Nima Ghorbani, Nikolaus F Troje, Gerard Pons-Moll, and Michael J Black. Amass: Archive of motion capture as surface shapes. In *Proceedings of the IEEE/CVF international conference on computer vision*, pages 5442–5451, 2019. 3
- [22] Denys Makoviychuk and Viktor Makoviychuk. rl-games: A high-performance framework for reinforcement learning. [https://github.com/Denys88/rl\\_games](https://github.com/Denys88/rl_games), 2021. 2
- [23] Viktor Makoviychuk, Lukasz Wawrzyniak, Yunrong Guo, Michelle Lu, Kier Storey, Miles Macklin, David Hoeller, Nikita Rudin, Arthur Allshire, Ankur Handa, and Gavriel State. Isaac gym: High performance gpu-based physics simulation for robot learning, 2021. 7
- [24] Jiageng Mao, Siheng Zhao, Siqi Song, Tianheng Shi, Junjie Ye, Mingtong Zhang, Haoran Geng, Jitendra Malik, Victor Guizilini, and Yue Wang. Learning from massive human videos for universal humanoid pose control. *arXiv preprint arXiv:2412.14172*, 2024. 2, 3
- [25] Meike Nauta, Doina Bucur, and Christin Seifert. Causal discovery with attention-based convolutional neural networks. *Machine Learning and Knowledge Extraction*, 1(1):19, 2019. 6

- [26] Soohwan Park, Hoseok Ryu, Seyoung Lee, Sunmin Lee, and Jehee Lee. Learning predict-and-simulate policies from unorganized human motion data. *ACM Transactions on Graphics (TOG)*, 38(6):1–11, 2019. 3
- [27] Xue Bin Peng, Glen Berseth, and Michiel Van de Panne. Terrain-adaptive locomotion skills using deep reinforcement learning. *ACM Transactions on Graphics (TOG)*, 35(4):1–12, 2016. 3
- [28] Xue Bin Peng, Glen Berseth, KangKang Yin, and Michiel Van De Panne. Deeploco: Dynamic locomotion skills using hierarchical deep reinforcement learning. *Acm transactions on graphics (tog)*, 36(4):1–13, 2017. 3
- [29] Xue Bin Peng, Pieter Abbeel, Sergey Levine, and Michiel Van de Panne. Deepmimic: Example-guided deep reinforcement learning of physics-based character skills. *ACM Transactions On Graphics (TOG)*, 37(4):1–14, 2018. 1, 3, 4, 5
- [30] Xue Bin Peng, Angjoo Kanazawa, Jitendra Malik, Pieter Abbeel, and Sergey Levine. Sfv: Reinforcement learning of physical skills from videos. *ACM Transactions On Graphics (TOG)*, 37(6):1–14, 2018. 2, 3, 5, 6, 8
- [31] Xue Bin Peng, Ze Ma, Pieter Abbeel, Sergey Levine, and Angjoo Kanazawa. Amp: Adversarial motion priors for stylized physics-based character control. *ACM Transactions on Graphics (ToG)*, 40(4):1–20, 2021. 3
- [32] Xue Bin Peng, Yunrong Guo, Lina Halper, Sergey Levine, and Sanja Fidler. Ase: Large-scale reusable adversarial skill embeddings for physically simulated characters. *ACM Transactions On Graphics (TOG)*, 41(4):1–17, 2022. 3
- [33] Huaijin Pi, Ruoxi Guo, Zehong Shen, Qing Shuai, Zechen Hu, Zhumei Wang, Yajiao Dong, Ruizhen Hu, Taku Komura, Sida Peng, et al. Motion-2-to-3: Leveraging 2d motion data to boost 3d motion generation. *arXiv preprint arXiv:2412.13111*, 2024. 2
- [34] Marc H Raibert and Jessica K Hodgins. Animation of dynamic legged locomotion. In *Proceedings of the 18th annual conference on Computer graphics and interactive techniques*, pages 349–358, 1991. 3
- [35] Daniele Reda, Hung Yu Ling, and Michiel Van De Panne. Learning to brachiate via simplified model imitation. In *ACM SIGGRAPH 2022 conference proceedings*, pages 1–9, 2022. 1
- [36] John Schulman, Philipp Moritz, Sergey Levine, Michael Jordan, and Pieter Abbeel. High-dimensional continuous control using generalized advantage estimation. *arXiv preprint arXiv:1506.02438*, 2015. 3
- [37] Agon Serifi, Ruben Grandia, Espen Knoop, Markus Gross, and Moritz Bächer. Robot motion diffusion model: Motion generation for robotic characters. In *SIGGRAPH Asia 2024 Conference Papers*, pages 1–9, 2024. 3
- [38] Tianxin Tao, Matthew Wilson, Ruiyu Gou, and Michiel Van De Panne. Learning to get up. In *ACM SIGGRAPH 2022 Conference Proceedings*, pages 1–10, 2022. 3
- [39] Chen Tessler, Yoni Kasten, Yunrong Guo, Shie Mannor, Gal Chechik, and Xue Bin Peng. Calm: Conditional adversarial latent models for directable virtual characters. In *ACM SIGGRAPH 2023 Conference Proceedings*, pages 1–9, 2023. 3
- [40] Guy Tevet, Sigal Raab, Brian Gordon, Yoni Shafir, Daniel Cohen-or, and Amit Haim Bermano. Human motion diffusion model. In *The Eleventh International Conference on Learning Representations*, 2022. 3
- [41] Guy Tevet, Sigal Raab, Setareh Cohan, Daniele Reda, Zhengyi Luo, Xue Bin Peng, Amit H Bermano, and Michiel van de Panne. Cload: Closing the loop between simulation and diffusion for multi-task character control. *arXiv preprint arXiv:2410.03441*, 2024. 3, 8
- [42] Aaron Van Den Oord, Oriol Vinyals, et al. Neural discrete representation learning. *Advances in neural information processing systems*, 30, 2017. 6
- [43] Marek Vondrak, Leonid Sigal, Jessica Hodgins, and Odest Jenkins. Video-based 3d motion capture through biped control. *ACM Transactions On Graphics (TOG)*, 31(4):1–12, 2012. 3
- [44] Bastian Wandt, James J Little, and Helge Rhodin. Elepose: Unsupervised 3d human pose estimation by predicting camera elevation and learning normalizing flows on 2d poses. In *Proceedings of the IEEE/CVF Conference on Computer Vision and Pattern Recognition*, pages 6635–6645, 2022. 2
- [45] Jiashun Wang, Yifeng Jiang, Haotian Zhang, Chen Tessler, Davis Rempe, Jessica Hodgins, and Xue Bin Peng. Hil: Hybrid imitation learning of diverse parkour skills from videos. *arXiv preprint arXiv:2505.12619*, 2025. 3
- [46] Yinhuai Wang, Qihan Zhao, Runyi Yu, Hok Wai Tsui, Ailing Zeng, Jing Lin, Zhengyi Luo, Jiwen Yu, Xiu Li, Qifeng Chen, Jian Zhang, Lei Zhang, and Ping Tan. Skillmimic: Learning basketball interaction skills from demonstrations. In *Proceedings of the Computer Vision and Pattern Recognition Conference (CVPR)*, pages 17540–17549, 2025. 3
- [47] Jungdam Won, Deepak Gopinath, and Jessica Hodgins. Physics-based character controllers using conditional vaes. *ACM Transactions on Graphics (TOG)*, 41(4):1–12, 2022. 3
- [48] Zhen Wu, Jiaman Li, Pei Xu, and C Karen Liu. Human-object interaction from human-level instructions. *arXiv preprint arXiv:2406.17840*, 2024. 3
- [49] Zeqi Xiao, Tai Wang, Jingbo Wang, Jinkun Cao, Wenwei Zhang, Bo Dai, Dahua Lin, and Jiangmiao Pang. Unified human-scene interaction via prompted chain-of-contacts. In *The Twelfth International Conference on Learning Representations*, 2024. 3
- [50] Kevin Xie, Tingwu Wang, Umar Iqbal, Yunrong Guo, Sanja Fidler, and Florian Shkurti. Physics-based human motion estimation and synthesis from videos. In *Proceedings of the IEEE/CVF International Conference on Computer Vision*, pages 11532–11541, 2021. 3
- [51] Sirui Xu, Zhengyuan Li, Yu-Xiong Wang, and Liang-Yan Gui. Interdiff: Generating 3d human-object interactions with physics-informed diffusion. In *Proceedings of the IEEE/CVF International Conference on Computer Vision*, pages 14928–14940, 2023. 3
- [52] Sirui Xu, Hung Yu Ling, Yu-Xiong Wang, and Liang-Yan Gui. Intermimic: Towards universal whole-body control for physics-based human-object interactions. *arXiv preprint arXiv:2502.20390*, 2025. 1, 3
- [53] Yufei Xu, Jing Zhang, Qiming Zhang, and Dacheng Tao. Vitpose: Simple vision transformer baselines for human pose

- estimation. *Advances in neural information processing systems*, 35:38571–38584, 2022. [7](#)
- [54] Heyuan Yao, Zhenhua Song, Baoquan Chen, and Libin Liu. Controlvae: Model-based learning of generative controllers for physics-based characters. *ACM Transactions on Graphics (TOG)*, 41(6):1–16, 2022. [3](#)
- [55] Heyuan Yao, Zhenhua Song, Yuyang Zhou, Tenglong Ao, Baoquan Chen, and Libin Liu. Moconvq: Unified physics-based motion control via scalable discrete representations. *ACM Transactions on Graphics (TOG)*, 43(4):1–21, 2024. [3](#)
- [56] Vickie Ye, Georgios Pavlakos, Jitendra Malik, and Angjoo Kanazawa. Decoupling human and camera motion from videos in the wild. In *IEEE Conference on Computer Vision and Pattern Recognition (CVPR)*, 2023. [8](#)
- [57] KangKang Yin, Kevin Loken, and Michiel Van de Panne. Simbicon: Simple biped locomotion control. *ACM Transactions on Graphics (TOG)*, 26(3):105–es, 2007. [3](#)
- [58] KangKang Yin, Stelian Coros, Philippe Beaudoin, and Michiel van de Panne. Continuation methods for adapting simulated skills. *ACM Trans. Graph.*, 27(3):1–7, 2008. [3](#)
- [59] Ri Yu, Hwangpil Park, and Jehee Lee. Human dynamics from monocular video with dynamic camera movements. *ACM Transactions on Graphics (TOG)*, 40(6):1–14, 2021. [2](#), [3](#)
- [60] Ye Yuan and Kris Kitani. Ego-pose estimation and forecasting as real-time pd control. In *Proceedings of the IEEE/CVF International Conference on Computer Vision*, pages 10082–10092, 2019. [5](#)
- [61] Ye Yuan, Shih-En Wei, Tomas Simon, Kris Kitani, and Jason Saragih. Simpoe: Simulated character control for 3d human pose estimation. In *Proceedings of the IEEE/CVF conference on computer vision and pattern recognition*, pages 7159–7169, 2021. [3](#), [5](#)
- [62] Haotian Zhang, Ye Yuan, Viktor Makovychuk, Yunrong Guo, Sanja Fidler, Xue Bin Peng, and Kayvon Fatahalian. Learning physically simulated tennis skills from broadcast videos. *ACM Transactions on Graphics (TOG)*, 42(4):1–14, 2023. [2](#), [3](#)
- [63] Jianrong Zhang, Yangsong Zhang, Xiaodong Cun, Shaoli Huang, Yong Zhang, Hongwei Zhao, Hongtao Lu, and Xi Shen. T2m-gpt: Generating human motion from textual descriptions with discrete representations. In *Proceedings of the IEEE/CVF Conference on Computer Vision and Pattern Recognition (CVPR)*, 2023. [2](#)

# Learning to Control Physically-simulated 3D Characters via Generating and Mimicking 2D Motions

## Supplementary Material

### A. Preliminary of Reinforcement Learning

We approach the single-view 2D motion tracking using reinforcement learning, which formulates a Markov Decision Process (MDP) defined by the tuple  $\mathcal{M} = (\mathcal{S}, \mathcal{A}, \mathcal{T}, \mathcal{R})$ , where  $\mathcal{S}$  represents states,  $\mathcal{A}$  actions,  $\mathcal{T}$  environment dynamics, and  $\mathcal{R}$  reward functions. The tracking controller is modeled as a policy  $\pi(a_t|s_t)$ , which samples actions  $\mathbf{a}_t \in \mathcal{A}$  based on the current state  $\mathbf{s}_t \in \mathcal{S}$ . We collect state-action-reward trajectories  $\tau = \{(\mathbf{s}_t, \mathbf{a}_t, r_t)\}_{t=1}^T$  in the simulator, following the policy's actions, the simulation dynamics  $\mathcal{T}(\mathbf{s}_{t+1}|\mathbf{s}_t, \mathbf{a}_t)$ , and the reward function  $r_t = \mathcal{R}(\mathbf{s}_t, \mathbf{a}_t)$ . The training objective is to learn an optimal policy  $\pi^*$  that maximizes the expected cumulative return  $R = \mathbb{E}_\pi [\sum_t \gamma^t r_t]$  over the collected trajectories.

### B. Implementation Details

#### B.1. Data Preprocessing

We adopt a pinhole camera model for reprojection computation, where each camera view  $C$  is parameterized by  $C = (R_C, \tau_C, f_C)$ , with  $R_C$  and  $\tau_C$  denoting the extrinsic rotation and translation, and  $f_C$  representing the intrinsic parameters.

For in-the-wild videos, we estimate the camera parameters  $C$  and the initial states  $s_0$  directly from the extracted 2D motion sequences. We jointly optimize the camera extrinsics and the 3D character poses by minimizing a reprojection loss, while keeping the intrinsics fixed. The resulting 3D poses are then used as the initial states for single-view tracking training. To avoid ground penetration, we include an additional regularization term that penalizes any body points falling below the ground plane.

#### B.2. Proprioceptive States Representation

The proprioceptive states  $o_{\text{prop}}$  consists of the following elements: root height  $\mathbf{h}_t \in \mathbb{R}$ , root velocity in the local coordinate frame  $\mathbf{v}_t \in \mathbb{R}^3$ , root angular velocity in the local frame  $\mathbf{w}_t \in \mathbb{R}^3$ , joint rotations in local joint coordinates  $\mathbf{q}_t \in \mathbb{R}^{6 \times J}$ , joint velocities in local joint coordinates  $\dot{\mathbf{q}}_t \in \mathbb{R}^{3 \times J}$ , and the Cartesian positions of key body links in the local root frame  $\mathbf{p}_t \in \mathbb{R}^K$ .

#### B.3. Algorithm of Adaptive State Initialization

The details of the proposed adaptive state initialization strategy are provided in Algorithm 1.

---

#### Algorithm 1 Initial State Distribution Update and Sampling

---

```

1: Input: Initial state distribution  $d(s_0)$ , Reference motion frames  $\mathbf{X} = \{\mathbf{x}_0, \dots, \mathbf{x}_T\}$ , Critic network  $V_\phi$ 
2: Output: Updated initial state buffer  $\mathcal{B}$ 
3: Initialize: Create state buffer  $\mathcal{B} = \{\mathcal{B}_t\}_{t=0}^T$ , where each  $\mathcal{B}_t$  is dedicated to frame  $\mathbf{x}_t$ .
4: 

---


5: function SAMPLEINITIALSTATE( $\mathcal{B}_t$ )
6:   Scores  $\leftarrow \{\text{Score}(s) \mid s \in \mathcal{B}_t\}$ 
7:   Probabilities  $\leftarrow \text{Normalize}(\exp(\beta \cdot \text{Scores}))$   $\triangleright \beta$  controls prioritization
8:   return Sample( $\mathcal{B}_t$ , Probabilities)
9: end function
10: 

---


11: function UPDATESTATEBUFFER( $\mathcal{B}$ , Rollouts)
12:   for each state  $\{s_t, \mathbf{x}_t\}$  at frame  $\mathbf{x}_t$  in Rollouts do
13:     CriticScore  $\leftarrow V_\phi(s_t)$   $\triangleright$  Estimate value/tracking performance
14:     if CriticScore > Threshold or  $|\mathcal{B}_t| < \text{MinSize}$  then
15:       Score( $s_t$ )  $\leftarrow$  CriticScore
16:        $\mathcal{B}_t \leftarrow \mathcal{B}_t \cup \{s_t\}$   $\triangleright$  Store state in the buffer for frame  $t$ 
17:       if  $|\mathcal{B}_t| > \text{MaxSize}$  then
18:          $\mathcal{B}_t \leftarrow \text{RemoveLowestScore}(s', \mathcal{B}_t)$   $\triangleright$  Maintain buffer size limit
19:       end if
20:     end if
21:   end for
22: end function

```

---

#### B.4. 2D Motion Tokenizer

We employ a VQ-VAE as the motion tokenizer. The VQ-VAE comprises an encoder  $E(\cdot)$  and a decoder  $D(\cdot)$ . The encoder converts the relative 2D motion sequence  $\mathbf{x}^{\text{rel}}$  into a sequence of lower-dimensional latent vectors,  $\mathbf{z} = [z_0, z_1, \dots, z_{T/l}]$ , where  $l$  denotes the temporal downsampling factor. Each latent vector  $z_i$  is then quantized to its nearest entry in a learned codebook of discrete embeddings  $\mathbf{C} = \{c_k\}_{k=1}^K$  by  $\hat{z}_i = \arg \min_{c_k \in \mathbf{C}} \|z_i - c_k\|_2$ .

The decoder reconstructs the original relative 2D motions from the quantized latent representations, i.e.,  $\hat{\mathbf{x}}^{\text{rel}} = D(\hat{\mathbf{z}})$ , where  $D(\cdot)$  denotes the decoder and  $\hat{\mathbf{z}}$  are the quantized latents.

The VQ-VAE is trained by minimizing the following loss



Table 4. Key Hyperparameters for the Policy Learning (PPO).

Hyperparameter	Value
Optimizer	Adam
Batch Size	16,384
Learning rate	$2 \times 10^{-5}$
Total Training Frames	$5 \times 10^{10}$
Number of Environments	16,384
Rollout Length	32
PPO Epochs ( $N_{\text{epochs}}$ )	3
Value Loss Coefficient	5
Discount Factor $\gamma$	0.99
GAE $\tau$	0.95
PPO clipping	0.2

function:

$$\mathcal{L}_{\text{vq}} = \mathcal{L}_{\text{recon}} + \|\text{sg}[\mathbf{Z}] - \hat{\mathbf{Z}}\|_2^2 + \beta \|\mathbf{Z} - \text{sg}[\hat{\mathbf{Z}}]\|_2^2, \quad (9)$$

where  $\mathcal{L}_{\text{recon}}$  is the reconstruction loss, the second term encourages the embedding vectors to be close to the encoder outputs, and the third term penalizes the encoder for deviating from the quantized embeddings. Here,  $\text{sg}[\cdot]$  denotes the stop-gradient operator, and  $\beta$  is a hyperparameter that balances the commitment loss. We stabilize training through exponential moving average (EMA) updates on codebook embeddings [63].

### B.5. Autoregressive Generator

We use a Transformer decoder architecture for the autoregressive generator to predict motion tokens. Each discrete token index is first mapped into an embedding, and a conditional embedding, which can be derived from the given control input or set to zero for unconditional generation, is prepended to the sequence. Absolute positional embeddings are added to encode the temporal order.

For generative tasks that are more sensitive to depth ambiguity in single-view 2D inputs, such as dance motion generation, we train a multi-view 2D generator to supply an additional viewpoint, helping to resolve missing depth cues. To construct training data for the multi-view generator, we collect 3D motion states from the simulated character while it tracks the original single-view 2D sequences, then project them into multiple 2D views to obtain paired multi-view motion samples. We represent the resulting multi-view 2D motions as sequential data, where each frame contains multiple motion tokens ordered by view ID.

### B.6. Key Hyperparameters

The key hyperparameters for policy learning are listed in Table 4. Our PPO implementation is based on RL-Games [22]. The hyperparameters for the VQ-VAE and

Table 5. Key Hyperparameters for the VQ-VAE Motion Tokenizer.

Hyperparameter	Value
<b>Training Configuration</b>	
Optimizer	Adam
Learning Rate	$5 \times 10^{-5}$
Batch Size	128
Training Steps	600,000
<b>Codebook Parameters</b>	
Codebook Size ( $K$ )	512
Embedding Dimension ( $D_{\text{embed}}$ )	128
<b>Architecture (ResNet Encoder/Decoder)</b>	
Model Width (Channels)	512
Number of ResNet Blocks	2
Temporal Downsampling Factor	2

Table 6. Key Hyperparameters for the Autoregressive Generator.

Hyperparameter	Value
<b>Training Configuration</b>	
Optimizer	Adam
Learning Rate	$5 \times 10^{-5}$
Batch Size	128
Training Steps	600,000
<b>Architecture (Transformer Decoder)</b>	
Transformer Layers ( $N_{\text{layers}}$ )	4
Attention Heads ( $N_{\text{head}}$ )	4
Embedding Dimension	256
<b>Data &amp; Sequence Parameters</b>	
Motion Clip Length (Frames)	60

the autoregressive generator are provided in Table 5 and Table 6, respectively.

## C. Additional Results

**State Initialization Strategy** We compare the learning curves of average tracking duration for a highly challenging animal jumping motion, with and without our proposed adaptive state initialization strategy. As shown in Fig. 8, our method enables effective convergence of policy learning, while the compared one struggles due to physically implausible initial states that hinder the training process.

**Impact of Multi-view Guidance** While our view-agnostic 2D tracking policy leverages diverse training viewpoints to acquire a robust 3D understanding, the inherent depth ambiguity of single-view inputs can still persist during inference for complex motions, causing irregular movements. To investigate this, we conducted an experiment us-

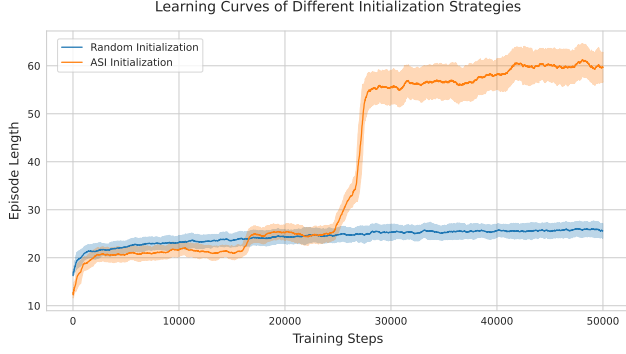


Figure 8. **Learning curve of 2D motion imitation with and without adaptive state initialization.** Adaptive optimization of the initial state distribution leads to significantly faster convergence in 2D motion imitation.

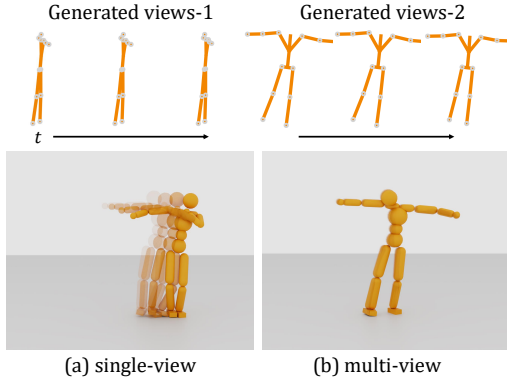


Figure 9. **Impact of multi-view guidance on resolving depth ambiguity.** Top: Reference keyframes generated from two view-points. Bottom: (a) Tracking guided only by View-1 results in instability and sliding due to depth ambiguity. (b) Tracking guided by both views successfully resolves these ambiguities, allowing the controller to recover stable and physically plausible 3D poses.

ing two orthogonal 2D reference views synthesized by our proposed 2D motion generator. We compared the policy’s performance when tracking only one of these views versus tracking both simultaneously. As illustrated in Fig. 9, the policy tracking a single generated view suffers from severe depth ambiguity, resulting in artifacts like foot sliding. In contrast, the policy integrating both views successfully resolves this ambiguity, maintaining stable poses and plausible motion.

## D. Limitation and Future Work

In our current approach, the 2D tracking policy relies exclusively on reprojection-error-based rewards. This geometric objective may be insufficient for learning precise contact dynamics required for fine-grained object interactions, such as dexterous manipulation or tool use. Future work could

address this by introducing additional semantic rewards to explicitly ground these contact constraints. Moreover, our framework currently assumes that camera parameters are estimated with reasonable accuracy. In practice, however, inaccurate camera estimation can significantly degrade the performance of the 2D tracking policy. To mitigate this, future iterations could incorporate camera parameters directly into the learning procedure, allowing for the joint optimization of motion control and camera estimation.